

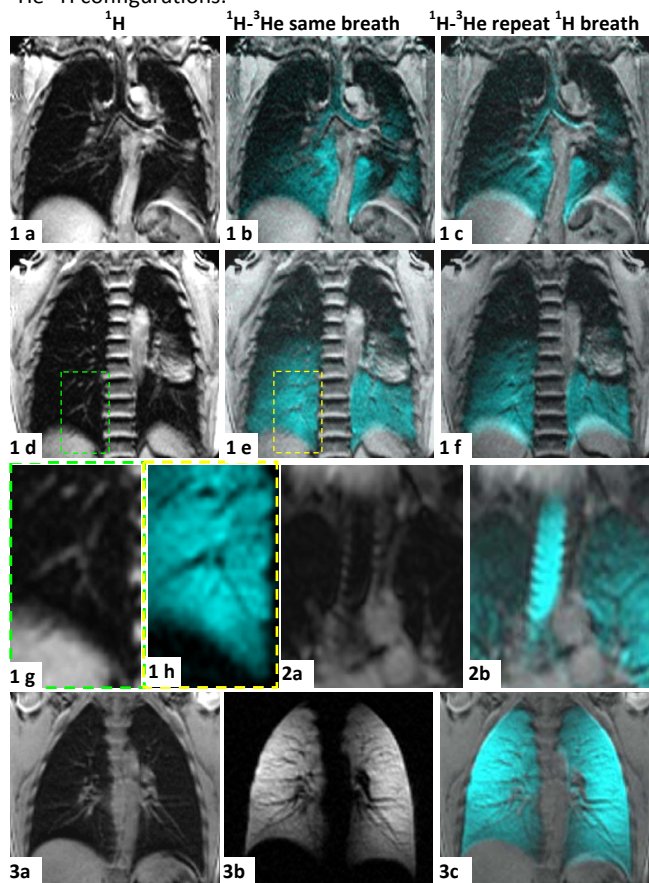
# Synchronised acquisition of hyperpolarised $^3\text{He}$ and $^1\text{H}$ MR images of the lungs during the same breath-hold

J. M. Wild<sup>1</sup>, S. Ajraoui<sup>1</sup>, M. H. Deppe<sup>1</sup>, S. R. Parnell<sup>1</sup>, H. Marshall<sup>1</sup>, J. Swinscoe<sup>2</sup>, M. Hatton<sup>2</sup>, J. Parra-Robles<sup>1</sup>, and R. H. Ireland<sup>1</sup>

<sup>1</sup>Academic Radiology, University of Sheffield, Sheffield, Yorkshire, United Kingdom, <sup>2</sup>Weston Park Hospital, Sheffield, United Kingdom

**Introduction** The combination of  $^1\text{H}$  MRI of lung anatomy with hyperpolarised gas MRI of lung function has previously required acquisition of separate breath-hold exams<sup>1,2</sup>, with separate MRI pulse sequences and dedicated RF coils, resulting in images that were not spatially registered or temporally synchronised. Retrospective image registration from different breath-holds can be performed, but residual errors remain<sup>3</sup> and the temporal synchronicity of any mutually interesting functional information<sup>4</sup> is lost. The synchronous detection of MR signals from different nuclei has been reported in the past with hardware for rapid switching between resonant frequencies, frequency multiplexed transmit and receive and dual tuned RF coils<sup>5-8</sup>. Nevertheless, no definitive clinical applications of synchronised dual resonance imaging have yet been demonstrated in-vivo. Here  $^1\text{H}$  anatomical and  $^3\text{He}$  ventilation MRI from human lungs were acquired in the same breath-hold using decoupled RF hardware and dual acquisition MRI pulse sequences. The effects of gradient non-linearity and background gradient dephasing for the two nuclei were investigated in flood phantom experiments at different FOVs. The resulting optimised  $^3\text{He}$  and  $^1\text{H}$  images acquired in the same breath were compared to those acquired in repeat breath-hold manoeuvres.

**Methods**  $^3\text{He}$  and  $^1\text{H}$  MRI was performed at 3T (Philips, Achieva) with rapid switching between 97 MHz and 128 MHz. A prototype linear Helmholtz coil (Pulseteq, UK) was used for  $^3\text{He}$  T-R, which was detuned with trap circuits during  $^1\text{H}$  transmit.  $^1\text{H}$  T-R was performed with the scanner  $^1\text{H}$  body coil (quadrature birdcage) which was also detuned during  $^3\text{He}$  T-R.  $^3\text{He}$  was polarised to ~20% with rubidium spin-exchange apparatus (GE) and  $^3\text{He}$  imaging was performed with ethics and regulatory approval. Three volunteers and a single patient with lung cancer and COPD performed  $^3\text{He}$ - $^1\text{H}$  MRI by holding their breath following inhalation of 300-400 ml of  $^3\text{He}$  mixed with 600 ml  $\text{N}_2$  from a 1 litre bag. Dual acquisition of  $^3\text{He}$  ventilation and  $^1\text{H}$  lung anatomy MRI was performed from the same slices in the same breath-hold with a 2-D spoiled gradient echo sequence. The sequence was optimised for sequential slice acquisition of  $^3\text{He}$  and  $^1\text{H}$ : FA = 8°, TE 1.3 ms, TR 5 ms, 5×15 mm slice, FOV 38 cm, 128×127 matrix, BW/pixel = 500 Hz. Repeated  $^1\text{H}$  images of lung anatomy were acquired following replication of the breath-hold manoeuvre by a repeat breath of 1 litre of air from the same bag. Spatial registration of the images was assessed by mutual overlap. To assess the effects of gradient linearity and image distortion from background  $B_0$  gradients, additional experiments were performed with the  $^1\text{H}$  FOV (38cm) and  $^3\text{He}$  FOV (50 cm) scaled in the ratio of their respective gyromagnetic ratios, such that pulse sequences had identical read and phase gradient strengths. These experiments were then repeated with  $^1\text{H}$  flood phantoms with gradient strengths and BW/pixel mimicking the  $^3\text{He}$ - $^1\text{H}$  configurations.



**Results & Discussion** Figure 1 shows example image slices acquired from the patient with lung cancer and COPD. The  $^1\text{H}$  anatomical images (1a & 1d) show evidence of tumour in the left lung and some infiltration around the main bronchi. The central images are the  $^3\text{He}$  MRI (1b & 1c) acquired in the same breath superimposed upon the  $^1\text{H}$ . The inherent spatial registration of the fine structure such as the pulmonary blood vessels (see enlarged  $^1\text{H}$  in 1g &  $^3\text{He}$  in 1h), trachea and bronchi is visible in the images. Moreover, the impeded ventilation in the  $^3\text{He}$  images can be related to the anatomical signs of airway constriction from the tumour in the registered  $^1\text{H}$  MRI although the obstructive effects of COPD may also play a part in the  $^3\text{He}$  heterogeneity. The  $^1\text{H}$  images in the right column (1c & 1f) were acquired in a subsequent replica breath-hold following a repeat inhalation of 1 litre of air from the bag. Note the mis-registration with the  $^3\text{He}$  MRI which is most visible at the lung bases and in the airways. Shown in 2a & 2b are magnified regions of the synchronised  $^3\text{He}$  and  $^1\text{H}$  images from one of the volunteers. Note the registered contours of the tracheal cartilage rings. Fig 3 shows example of the images from the second volunteer with excellent  $^3\text{He}$ - $^1\text{H}$  spatial registration. From the experiments conducted at different FOV (not shown for space) we conclude that the only source of image mis-registration is gradient non-linearity and different levels of inter-pixel dephasing from background gradients resulting from the different  $\gamma$  of the nuclei.

**Conclusion** Spatially registered concurrent acquisition of lung MRI from two different nuclei is demonstrated in-vivo. The temporal and spatial registration of these images is shown to be superior to that achievable in separate scans with repeated breath-hold manoeuvres. The current implementation acquired  $^1\text{H}$  and  $^3\text{He}$  slices sequentially with a 0.6 s delay, the synchronicity could be improved by interleaving between the nuclei per RF view which is currently under implementation, or with simultaneous excitation with dual frequency RF pulses<sup>7</sup>. The synchronised nature of the dual acquisition method has multiple applications in both static and dynamic lung MRI allowing side by side quantitative analysis of impaired lung function from the  $^3\text{He}$  images and anatomical signs of disease from  $^1\text{H}$  MRI. The mutual information from the registered  $^1\text{H}$  MRI may also aid in improving the subsequent registration of the hyperpolarised MRI to CT and other imaging modalities<sup>3</sup>.

**References** <sup>1</sup>Journal of Magnetic Resonance Imaging 21, 365 (2005). <sup>2</sup>Radiology 212, 885 (1999). <sup>3</sup>Phys Med Biol 53, 6055 (2008). <sup>4</sup>Magn Reson Med 57, 1185 (2007). <sup>5</sup>Magma 4, 187 (1996). <sup>6</sup>Magn Reson Med 52, 693 (2004). <sup>7</sup>Magn Reson Imaging 4, 343 (1986). <sup>8</sup>Magn Reson Med 28, 300 (1992).

**Acknowledgements** GE for polariser support, EPSRC grant #EP/D070252/1, EU FP6, Philips Medical Systems.